Published in final edited form as:
Eur J Nucl Med Mol Imaging. 2014 May ; 41(5): 934–945. doi:10.1007/s00259-013-2653-y.

Arterial and Fat Tissue Inflammation are Highly Correlated - A Prospective ^{18}F-FDG PET/CT Study

Jan Bucerius, MD[1,2,3,4,5], **Venkatesh Mani, PhD**[1,2,6], **Stephanie Wong**[1,2], **Colin Moncrieff**[1,2], **David Izquierdo-Garcia, PhD**[1,2], **Josef Machac, MD**[7], **Valentin Fuster, MD, PhD**[6,8], **Michael E. Farkouh, MD, MSc**[6,9], **James H. F. Rudd, MD, PhD**[10,*], and **Zahi A. Fayad, PhD**[1,2,6,*]

[1]Translational and Molecular Imaging Institute, Mount Sinai School of Medicine, New York, New York [2]Department of Radiology, Mount Sinai School of Medicine, New York, New York [3]Department of Nuclear Medicine, Maastricht University Medical Center, Maastricht; The Netherlands [4]Cardiovascular Research Institute Maastricht (CARIM), Maastricht University Medical Center, Maastricht; The Netherlands [5]Department of Nuclear Medicine, University Hospital RWTH Aachen, Aachen; Germany [6]Department of Cardiology, Zena and Michael A. Weiner Cardiovascular Institute and Marie-Josée and Henry R. Kravis Cardiovascular Health Center, Mount Sinai School of Medicine, New York, New York [7]Division of Nuclear Medicine, Department of Radiology, Mount Sinai School of Medicine, New York, New York [8]The Centro Nacional de Investigaciones Cardiovasculares (CNIC), Madrid; Spain [9]Cardiovascular Imaging Clinical Trials Unit, Mount Sinai School of Medicine, New York, New York [10]Division of Cardiovascular Medicine, University of Cambridge, Cambridge; United Kingdom

Abstract

Purpose—There is evidence that the link between obesity and cardiovascular disease might relate to inflammation in both fat tissue and the arterial wall. ^{18}F-fluorodeoxyglucose positron emission tomography (FDG-PET) uptake is a surrogate marker of vessel wall inflammation. The aim of the study was to measure FDG uptake in both regions using PET and identify links between adipose and arterial inflammation.

Methods—173 cardiovascular patients were prospectively imaged with FDG-PET/CT. Arterial FDG uptake was measured in the carotid arteries and ascending aorta. The same was done in fat tissue in the neck, the pre-sternal region (all subcutaneous) and the pericardium. FDG uptake wasquantified as average maximal target-to-background ratio ($_{mean}TBR_{max}$).Multivariate regression analyses were performed to identify significant associations between arterial and adipose tissue FDG uptake and clinical variables as given by the standardized correlation coefficient (β).

Results—FDG uptake values within all fat tissue regions were highly predictive of vascular FDG uptake in both the carotids (neck subcutaneous: β:0.262, $p<0.0001$) and aorta (chest pericardial: β:

Corresponding Author: Zahi A. Fayad, PhD, Director, Translational and Molecular Imaging, Institute, Mount Sinai School of Medicine, One Gustave L. Levy Place, P. O. Box 1234, New York, NY 10029; USA, zahi.fayad@mssm.edu.
*J. H. F. R and *Z. A. F contributed equally to this work and are joint senior authors.

Conflict of interest statement:
The authors declare that they have no conflict of interest.

0.220, p=0.008 and chest subcutaneous: β:0.193, p=0.019). Obesity was significantly associated with elevated FDG uptake in adipose tissue (neck subcutaneous: β:0.470, p<0.0001; chest subcutaneous: β:0.619, p=0.028; chest pericardial: β:0.978, p=0.035).

Conclusion—FDG uptake in diverse fat tissue regions was significantly associated with arterial FDG uptake, a reasonable surrogate of inflammation. Increasing body weight significantly predicted the level of fatty inflammation. FDG-PET therefore provides imaging evidence for an inflammatory link between fat tissue and the vasculature in patients with cardiovascular disease.

Keywords

FDG-PET; Inflammation; Atherosclerosis; Fat Tissue; Carotid Arteries; Aorta

INTRODUCTION

Obesity, the most common nutritional disorder in industrial countries, is associated with increased cardiovascular mortality and morbidity [1–4]. Recent data suggest that metabolic and cardiovascular disease in human obesity is mediated by inflammation of adipose tissue driven by monocyte / macrophage infiltration and overproduction of proatherogenic cytokines [5–7]. Furthermore, chronic activation of the immune system has been strongly implicated in the pathogenesis of obesity-associated disorders, including type 2 diabetes mellitus and cardiovascular disease, and is a growing target of interest for therapeutic intervention [5,8].It is also likely that pro-inflammatory changes in fat tissue are linked to vascular endothelial dysfunction [2].Supporting this pathophysiologic link, several previously published studies have demonstrated that the accumulation of fat around the heart is associated with an increased risk of both coronary artery disease (CAD) and vascular calcification [9–13]. However, the underlying mechanisms of this association remain unknown [9].

^{18}F-fluordeoxyglucose positron emission tomography (FDG-PET) reflects the metabolic rate of glucose, a process known to be enhanced in inflamed tissue. Vascular FDG uptake has been shown to be significantly associated with both the degree of macrophage infiltration and the levels of inflammatory gene expression in atherosclerotic plaque [14–16].Likewise, FDG-PET can also non-invasively image the metabolic activity in visceral and subcutaneous fat tissue and might therefore serve as a surrogate marker of fat tissue inflammation [17,18]. Previously published studies investigating the impact of cardiovascular risk factors on vascular FDG uptake revealed that obesity and the metabolic syndrome were among the most important risk factors for vascular inflammation [4,19,20]. However, no data have been published so far about the potential link between the FDG uptake in the fat tissue and that in the vasculature.

Therefore, the aim of this study was to evaluate whether the degree of FDG uptake in different fat tissue regions (FTRs) is linked to FDG uptake in the carotid arteries and aorta and, furthermore, to identify cardiovascular risk factors that might be associated with elevated arterial and fat tissue FDG uptake.

PATIENTS AND METHODS

Study Design

This was a prospective imaging study, investigating the impact of the FDG uptake in different FTRs on the prevalence of carotid-and aortic wall inflammation assessed by FDG-PET. This study, approved by the institutional review board, was conducted from February 2006 until April 2011 at the Mount Sinai School of Medicine, New York, U.S.A. All subjects gave written informed consent.

Criteria for inclusion in the study were as follows: Males and females with a diagnosis of cardiovascular disease or with multiple cardiovascular disease risk factors were recruited. Definition of cardiovascular disease was previous myocardial infarction, stroke, transient ischemic attack, history of peripheral artery disease or a history of a coronary revascularization procedure. Patients with fasting glucose levels ≥ 11.1 mmol/l, previous carotid surgery, known vasculitis and / or malignancies were excluded from the study. Patients with the incidental finding of, previously unknown, vasculitis on the PET scan were excluded from further analyses.

Questionnaire, Biometric and Biochemical Measurements

We assessed the presence of cardiovascular risk factors, use of medication, and family history of cardiovascular disease by using a questionnaire. Presence of hypertension was defined as a history systolic blood pressure > 140 mmHg, or a diastolic blood pressure > 90 mmHg. Diabetes was defined as documented diagnosis of type 1- or -2 diabetic disease and the use of anti-diabetic treatment (diet, oral- or insulin treatment). Weight and height were measured to calculate body mass index (BMI). Smoking was defined as smoking at least one cigarette on a daily basis. Fasting glucose levels were obtained by finger stick blood glucose measurements (Accu-Chek™ Advantage™, Roche Diagnostics; Indianapolis, Indiana) prior to FDG administration.

FDG-PET/CT Imaging

FDG-PET/CT was performed after an overnight fast using a General Electric Healthcare (Milwaukee, Wisconsin) Lightspeed discovery™ ST 16-slice PET/CT scanner. FDG was administered intravenously (558.7 ± 96.2MBq) and patients rested comfortably for approximately 90 to 120 min. To exclude any impact of the outside temperature on the fat tissue assessment with FDG-PET, i. e. activation of brown fat tissue, we assured that room temperature in the room where patients were injected and afterwards waiting until the start of the PET acquisition was consistent during summer and winter time. Furthermore, patients were admitted to the PET facility couple of hours before FDG was injected because of the administrative work, including assessment of height and weight of the patients, taking the history of the patients, etc., which had to be done before the PET study. At the time of the FDG injection, patient's body temperature was therefore appropriately adopted to the room temperature.

Imaging of the ascending aorta was performed first and covered the area from the heart to the aortic arch as the upper limit, over 15–30 min (1 or 2 bed positions) acquisition time

depending on the patient's anatomy. Afterwards, subjects were placed into a head holder for imaging of the carotids. Images from one bed position (15.5 cm) with coverage extending inferior to the internal auditory meatus were acquired for 15 minutes. We chose two separate acquisitions so we could improve the image quality with arms up for the aorta acquisition and arms down for the carotid acquisition.

A low dose CT scan (140 kV, 80 mA, and 4.25 mm slice thickness) was performed for attenuation correction and co-registration. No CT contrast agent was administered. The absence of CT contrast was deliberate, to allow those with renal impairment to be imaged. The main studies of reproducibility also did not use contrast CT, but nevertheless reported excellent reproducibility [4,21].

Image Analysis of the Vessels

Image analysis was performed on a dedicated commercially available workstation (Extended Brilliance™ Workspace V4.0.0.3206; Philips Medical Systems Inc.; Cleveland, Ohio). One experienced reader (J. B.) analyzed all scans.

Methodology for analysis and reproducibility of the measurements have been previously reported in detail [4]. Briefly, arterial FDG uptake was quantified by manually drawing a region of interest (ROI) around each common carotid artery and the ascending aorta, including the vessel lumen, on every slice of the co-registered transaxial PET/CT images. Next, the maximum arterial standardized uptake value (SUV) (highest pixel activity within the region of interest) was determined. The SUV is the decay-corrected tissue concentration of FDG in kBq/ml, adjusted for the injected FDG dose and the body weight of the patient. By averaging the maximum SUV values of all arterial slices of the left and right carotid artery and the ascending aorta, respectively, a $_{mean}SUV_{max}$ value was derived for all arteries.

The arterial target-to-background ratio (TBR) was calculated by normalizing the arterial SUV for blood pool activity by dividing the SUV values in the arteries by the average blood mean SUV estimated from both jugular veins (carotid SUV values)or the superior vena cava (aortic SUV values), respectively. Choosing the two different veins most optimal reflects the respective FDG blood pool activity at the time of the aortic or carotid data acquisition, respectively, because obviously each of them was scanned in the respective field of view with the corresponding artery. FDG blood pool analysis was done by placing at least six 3–4 mm ROIs in consecutive slices of the respective vein and averaging the obtained mean SUV values. The TBR is a blood-normalized arterial SUV, considered to be a reflection of arterial FDG uptake and reflective of underlying macrophage activity [22]. The arterial TBR values obtained were then averaged in order to derive a $_{mean}TBR_{max}$ for both carotid arteries and the ascending aorta.

Image Analysis of the Fat Tissue

FTRs, defined as subcutaneous fat tissue in the neck (NeckSub) and in the presternal area (ChestSub)as well as pericardial fat tissue (ChestPeri) were identified based on pre-defined ranges of Hounsfield units (HU) of −70 to −110 from CT images as previously described[17]. After CT fusion with the PET images, ROIs were placed on three consecutive

slices whenever possible and mean and maximal SUV values across those slices were averaged (Figure 1).To reduce the possibility of FDG uptake by brown fat tissue and / or physiological FDG uptake into the myocardium on the FDG uptake values of the different FTRs, ROIs were placed away from regions of fat tissue with focally increased FDG uptake or in regions with diffusely increased FDG uptake with SUVs close to or above of 1.5, which are usually considered to reflect brown fat tissue[23]. A cutoff SUV of 2.0 represented the lower boundary of activity in patients with detectable brown adipose tissue according to a recently published study about the method of FDG uptake into brown fat tissue, and it was seen to be more than 2 standard deviations above the maximal SUV seen in typical depots of white adipose tissue [23]. However, to exclude an impact of the FDG uptake into brown fat tissue on the subcutaneous- and pericardial white fat tissue ROIs to the highest degree, we decided to even lower that cutoff to a SUV of 1.5 and not to place ROIs in fat tissue regions with a FDG uptake close to this threshold.

ROIs in the pericardial fat region were placed in the substernal mediastinal region of the chest cranial of the heart and therefore as far away as possible from the myocardium and the large vessels (e. g. the aortic arch) in order to exclude overspill from the myocardial and / or vascular FDG uptake into the pericardial fat tissue region (Figure 1, middle). Furthermore, ChestPeri ROIs were not placed at all if such an overspill could not be excluded to the highest possible degree. As this was rarely the case, mainly in patients with a pretty high myocardial FDG uptake, in approximately 90% (88.4%, Table 2) of cases pericardial fat tissue ROIs could be appropriately placed without the suspicion for an overspill from any vascular and / or myocardial FDG uptake. ROI diameters for all fat tissue regions were at least above 6 mm. As for the vascular SUV values, fat tissue SUVs of the neck region were corrected by the blood pool activity of the jugular veins, and the two other FTRs by SUV values of the superior vein cava in order to obtain fat tissue TBR values, which we assume to reflect the true metabolic activity and / or the inflamed state of fat tissue cells.

Statistical Analysis

All continuous variables are expressed as mean ± standard deviation and categorical data as absolute numbers and percentages throughout this manuscript. In general, normal distribution of data was tested for all of the different statistical calculations using the Kolmogorov-Smirnov-Test. Comparison between the FDG uptake parameters of the different FTRs was performed using ANOVA with appropriate correction for multiple comparisons using Tukey post-hoc testing.

MULTIPLE REGRESSION WITH BACKWARD ELIMINATION AND LINEAR REGRESSION WITH ENTER METHOD—Multiple linear regression analyses with backward elimination was used to assess the association between the cardiovascular risk factors including the FDG uptake values in all FTRs and the vascular FDG uptake parameters ($_{mean}TBR_{max}$ values for both). $Vascular_{mean}TBR_{max}$ values were treated as the response variables (dependent) and the cardiovascular risk factors as the explanatory (independent) variables for the regression analysis. The explanatory variables included were as follows: age, male gender, body mass index (BMI), diabetes, history of cardiovascular disease, smoking, alcohol use, hypertension, family history of cardiovascular disease and the

FTRs$_{mean}$TBR$_{max}$ values. Following this, the ENTER regression was used to determine independent predictors of the response variables. For this method, all of the explanatory variables of the backward elimination model that showed a significant association with the vascular$_{mean}$TBR$_{max}$ value ($p < 0.10$) were retained and entered the regression model in a block in a single step. This entry method was preferred over the forward selection of variables since after excluding all of the explanatory variables without a significant association with the carotid- or aortic $_{mean}$TBR$_{max}$ value, respectively, only few significant variables were left for a relatively low number of cases. Throughout the manuscript, all results of the multiple regression models are provided with the standardized regression coefficient (β), the 95% confidence interval, and the p-value for the estimate of the statistical significance.

In order to identify potential associations between clinical variables and the FDG uptake in the different FTRs, age, BMI, hypertension, male gender, diabetes, smoking, and alcohol use served as explanatory variables while the$_{mean}$TBR$_{max}$value in the respective FTR was treated as the dependent variable. To more specifically evaluate the impact of the body habitus on the degree of FDG uptake in the fat tissue, we calculated the body surface area (BSA) for each individual patient following the duBois formula ($0.20247 * \text{height (m)}^{0.725} * \text{weight (kg)}^{0.425}$, BSA duBois) as well as the percent deviation from the individual normal Broca value (body height (cm) - 100; deviation: ((body weight (kg) * 100) / individual normal Broca value)-100)) [24]. Both variables entered the regression analyses as explanatory variables as well.

All statistical analyses were performed using SPSS™ statistical package 16.0 (SPSS Inc.; Chicago, Illinois).

RESULTS

Population Characteristics

One hundred seventy-three patients were included in the study. Table 1a shows characteristics of the study population. Numbers of patients in whom the different FDG uptake analyses of the carotid and aortic vessel walls and the FTRs could be performed are shown in Table 1b.

Exclusion of patients for distinct parts of the FDG uptake analyses was due to FDG uptake spill over from surrounding tissues and / or the inability to adequately place the ROI within the target tissue.

FDG-PET Imaging Results

The imaging analyses are given in Table 1b. ChestPeri $_{mean}$TBR$_{max}$values were significantly higher compared to the respective FDG uptake parameters of the other two FTRs ($p < 0.0001$ for all comparisons). No further statistically significant differences of the FDG uptake values between the different FTRs were observed.

Risk Factors for Increased Vascular FDG Uptake

Table 2 shows the results of the multiple linear regression analyses to identify clinical risk factors associated with FDG uptake parameters (i.e. measures of plaque inflammation) of the carotids and the ascending aorta. After retaining the significant explanatory variables from the backward elimination model, FDG uptake in the NeckSub region was significantly associated with the $_{mean}TBR_{max}$values of the carotids in the ENTER regression model (Table 2 + Figure 2 a). Accordingly, age, male gender, and history of cardiovascular disease were found to be significantly associated with the FDG $_{mean}TBR_{max}$ values in the carotids. Furthermore, a significantly negative association with diabetes was seen in the ENTER regression model.

With regard to the aorta, after retaining the significant explanatory variables ($p < 0.10$) from the backward model within the ENTER regression model, ChestPeri $_{mean}TBR_{max}$, ChestSub $_{mean}TBR_{max}$, BMI, and male gender showed a significant association with the $_{mean}TBR_{max}$ of the aorta (Table 2 + Figure 2 b).

Risk Factors for Increased Fat Tissue FDG Uptake

After retaining the variables significantly ($p < 0.10$) associated with the FDG uptake in the different FTRs from the initial backward regression model, ENTER regression model revealed BSA duBois to be significantly associated with NeckSub $_{mean}TBR_{max}$–, and ChestSub $_{mean}TBR_{max}$ values (Table 3). In contrast, BSA duBois did not show any statistical significant association with the ChestPeri $_{mean}TBR_{max}$. However, deviation from the normal Broca values was indeed the only significant risk factors for the intrathoracic fat tissue FDG uptake. It was also shown, that diabetes was negatively associated with the ChestPeri $_{mean}TBR_{max}$ values. This was indeed also the case for the BMI values showing a significantly negative association with the NeckSub $_{mean}TBR_{max}$ (Table 3).

DISCUSSION

The aim of our study was to determine if the degree of FDG uptake in different FTRs showed a significant association with vessel wall inflammation in the carotid arteries and aorta as depicted by FDG-PET/CT in a population of patients with known cardiovascular disease or multiple risk factors for it. Furthermore, we tried to identify clinical variables significantly associated with increased FDG uptake in the FTRs. We prospectively performed FDG-PET imaging in a large sample population with protocols optimized for vessel wall FDG uptake [22,25].

Our results demonstrate that the FDG uptake in different FTRs was significantly associated with the $_{mean}TBR_{max}$in the carotid- and the aortic wall. Additionally, we showed that increasing body weight, as depicted by BSA values and abnormally increased deviations from the normal Broca value, was the most important risk factor for the $_{mean}TBR_{max}$ in different FTRs. Surprisingly, we also found a negative association between BMI and the $_{mean}TBR_{max}$values in the NeckSub, a fact which we cannot finally explain, mainly because of the positive and highly significant correlation of the two other body mass parameters (BSA, Broca value) and the FDG uptake in those FTRs. However, these findings

might indeed reflect the known phenomenon called "obesity paradox" which accounts for a decreased cardiovascular risk with increased BMI values and which might be more pronounced in body regions with a higher fat burden such as the abdomen. Additionally, it might also reflect the fact that the BMI is not the most optimal surrogate marker for pathological overweight as it lacks of discriminatory power to differentiate between body fat and lean mass[26].

Rationale for Evaluating Fat Tissue FDG Uptake

Most clinical studies to date have used volumetric quantification of fat depots by CT or magnetic resonance imaging to evaluate associations with cardiovascular risk [11–13,17]. However, a preliminary report by Brunken et al. suggested that volumetric measurements alone may not be sufficient, and could be improved by using functional imaging with PET to determine the metabolic activity in fat tissue[17,27]. Furthermore, functional differences between subcutaneous and visceral fat tissue are well known [28]. For example, genes for angiotensinogen (blood pressure regulation), complement factors, and fatty acid-binding protein 4 (involved in fatty acid trapping in adipocytes), are expressed at higher levels in visceral adipose tissue than in subcutaneous fat[28–30]. These differences were highlighted in a study by Christen et al., in which higher FDG uptake values were shown in visceral than subcutaneous adipose tissue, implying higher metabolic activity within visceral fat [17].Furthermore, earlier studies by Virtanen et al. also showed higher rates of glucose uptake in visceral compared to subcutaneous adipose tissue in groups of healthy and diabetic men under euglycemic conditions[18,31]. Those findings are comparable with the results of the current study, as we found significantly higher FDG uptake values in pericardial fat tissue compared to the two different subcutaneous FTRs. Christen et al. also attempted to identify the cellular and molecular mechanisms underlying differential fat tissue glucose uptake. They noted increased glucose uptake within stromal regions taken from visceral adipose tissue compared to those from subcutaneous adipose tissue [17]. These stromal areas are known to contain inflammatory cells such as macrophages and T cells. Christen et al. suggested that the increase in glucose uptake in visceral adipose tissue might be explained by the increased expression of HK-1 (hexokinase-1, an enzyme facilitating phosphorylation of glucose) in visceral adipose tissue derived stromal vascular cells [17]. Interestingly, despite the well-known association between obesity and inflammation, no difference in FDG uptake in visceral adipose tissue was found between lean and obese individuals in their study. Another supportive paper was published by Elkhawad et al. in 2012.In a similar CVD population to the one described in our study, these authors found higher baseline FDG uptake values in visceral compared to subcutaneous fat tissue. In addition, there was also a more profound reduction in uptake of FDG in visceral fat tissue than subcutaneous following high-dose treatment with losmapimod, a p38 mitogen-activated protein kinase inhibitor [32].

Fat Tissue FDG Uptake and Carotid and Aortic Wall Inflammation

We found FDG uptake in the different FTRs the most consistent and among the most important risk factors for vascular FDG uptake, both in the carotids as well as in the aorta. As expected and in part previously reported by our group, diabetes showed negative associations with some of the vascular and FTR FDG uptake parameters, a fact, which might

most likely be due to a competitive effect between increased glucose levels in those diabetic patients and the FDG uptake in the vessels [20].

Prospective cohort studies as well as national surveys have shown that obese individuals have an increased risk for several adverse health outcomes, notably hypertension, diabetes, cardiovascular disease, arthritis, disability, as well as mortality. With regard to cardiovascular disease, it has also been shown that mean intima media thickness of internal carotid arteries, a marker of atherosclerosis, increases with increasing BMI [33,34]. Furthermore, significant associations exist between, body weight, presence of metabolic syndrome and vascular FDG uptake [4,19].

Though obesity has been characterized as a chronic inflammatory disease and atherosclerosis is now widely accepted as a vascular inflammatory disorder, scientific focus has only recently started to focus on the underlying mechanisms linking obesity and atherosclerosis. These mechanisms are however still poorly understood [30]. In contrast, monocytes and monocyte-derived macrophages are well known to be the cellular hallmarks in the pathogenesis of atherosclerosis [36]. Recently, animal studies have demonstrated a specific contribution of certain monocyte subsets to atherogenesis and, additionally, an obesity-associated macrophage accumulation in adipose tissue [37–39]. Furthermore, it was also shown that patients with coronary artery disease had a shift in monocyte subsets towards CD16+ monocytes compared to healthy controls[40]. These findings indicate for the first time a common role of CD16+ monocytes in the pathogenesis of obesity and atherosclerosis. The recently published I LIKE HOMe study revealed a significant association between counts of CD16+ monocytes with both obesity as well as subclinical atherosclerosis in a large cohort of healthy individuals [35]. This association between CD16+ monocytes and obesity confirms previously published results showing a shift towards CD16+ monocytes in morbidly obese patients [41]. In another study also published in 2010, Wu et al. found CD11c, a member of the β2-integrins, to be increased in obese humans with metabolic syndrome compared to lean controls [42,43]. The results of the current study seem to confirm these data, as we found deviations from the normal individual body weight, as depicted by increasing BSA- and abnormal Broca values, being the only variable consistently showing a significant association with the FDG uptake in all of the different FTRs.

CD11c increases monocyte adhesion to inflamed endothelial cells and has been used as an activation marker for monocytes/macrophages [44]. Furthermore, CD11c+ leukocytes in adipose tissue of mice have shown pro-inflammatory characteristics of classically-activated macrophages [45]. Blood monocyte CD11c has been shown to increase in hyperlipidemia and to play an important role in the development of atherosclerosis in apolipoprotein E-deficient mice [43]. The functional consequence of increased CD11c on adipose tissue leukocytes and blood monocytes in obesity may be related to an enhanced accumulation and/or activation of macrophages and/or dendritic cells in both adipose tissue and the arterial wall. This may contribute to T-cell accumulation and activation, thereby accelerating adipose tissue inflammation and atherogenesis, and contributing to the higher risk for atherosclerotic cardiovascular disease in obese individuals[42].The most recently published data by Hirata et al. are in line with this as they found a significantly enhanced infiltration of

macrophages and expression of pro- and anti-inflammatory cytokines in epicardial fat of patients with CAD compared with that in non-CAD patients [46]. Additionally, the ratio of M1/M2 macrophages was positively correlated with the severity of CAD. Furthermore, the expression of pro-inflammatory cytokines was positively correlated, and the expression of anti-inflammatory cytokines was negatively correlated with the ratio of M1/M2 macrophages in epicardial adipose tissue of CAD patients. By contrast, there was no significant difference in macrophage infiltration and cytokine expression in subcutaneous adipose tissue between the CAD and non-CAD groups. The results of our study in part confirm their results as we found a significant association between pericardial fat tissue FDG uptake and vascular FDG uptake in the aorta.

Limitations

With regard to the FDG uptake in the FTRs, we cannot totally exclude an impact of high insulin levels, as frequently seen in obese subjects with increased blood glucose levels, on the degree of fat tissue FDG uptake as described after insulin stimulation by Virtanen et al. [18]. However, we did not have patient's insulin levels available in the current study but we did not see any correlation between patients fasting glucose- and the BMI values (data not shown). This therefore should lower the impact of increased insulin levels as a reason for increased fat tissue FDG uptake in obese patients to some degree. Nevertheless, this issue needs clearly to be addressed in future studies.

As we did not use contrast-enhanced CT in the current study, soft plaques in the vessels could not be detected. The absence of CT contrast was deliberate, to allow those with renal impairment to be imaged. However, by intention, we chose a population either with defined atherosclerosis (e. g. known CAD, carotid artery disease, etc.) or multiple risk factors for it, and we included all evaluable slices of the arterial wall. Thereby, both focal and diffuse areas of FDG uptake have been included in the analysis. Furthermore, subjects with known vasculitis were excluded, and we made the assumption that any FDG signal within the vessel wall was likely to be due to accumulation of the tracer within atherosclerotic plaque. Others have previously demonstrated co-localization between lipid-rich plaque and FDG uptake [47].

Several further limitations of our study need to be addressed. Firstly, we did not obtain serum lipid levels, markers of glucose metabolism or serum inflammatory markers. Mainly regarding the latter point, markers such as hs-CRP and Lp-PLA2 would have given more information whether the link between fat and vascular FDG uptake reflects a more systemic pro-inflammatory state or a fat-specific phenomenon. As we did not find any association between statin therapy and vascular or fat tissue FDG uptake in our patient population (data not shown) a trend towards a more fat-specific phenomenon has at least to be considered. However, this has to be addressed in a future study.

As we mainly intended to evaluate the pericardial- compared to different subcutaneous FTRs, we are also lacking data on the FDG uptake in abdominal visceral FTRs. Secondly, it is unknown if fat tissue FDG uptake is predictive of progression of vascular disease or future cardiovascular events.

We are aware of the fact, that a potential overspill of the FDG uptake in surrounding tissues might impact the FDG uptake in the different fat tissue ROIs. This is mainly due for the pericardial fat tissue analysis, which might be affected by the physiological FDG uptake into the myocardium. However, as described in the methods section, we placed the fat tissue ROIs as far away from other structures as possible and skipped placing those ROIs in case we could not exclude an overspill at the highest degree. Furthermore, we used well accepted FDG uptake thresholds to exclude placing ROIs into brown fat tissue regions instead of into white fat tissue as indicated [23]. We also avoided an impact of the outside temperature on the fat tissue assessment with FDG-PET with respect to brown fat tissue activation. However, because analysis of fat tissue FDG uptake is an emerging field with pretty few data available, future studies clearly need to address the issue of most optimally placing ROIs for quantification of fat tissue metabolic activity as depicted by FDG-PET.

By intention, we decided to just analyze the ascending aorta instead of the whole or additional parts of the aorta. This was mainly due to the previously shown higher reproducibility of that part of the aorta but also in order to reduce the radiation exposure to the patients as much as possible[21].

CONCLUSION

In the current study, we show that fat tissue FDG uptake has a significant association with the FDG uptake in the wall of the ascending aorta and carotid arteries. Furthermore, increased body weight was the most important and consistent risk factor for FDG uptake in all fat tissue regions. Based on these results, FDG PET/CT seems to be capable of non-invasively imaging the well-known link between inflammatory fat tissue and vessel wall inflammation.

Acknowledgement

The authors wish to thank Ash Rafique, RT, BS, CNMT for his assistance with the image acquisition.

Work in this paper was partly supported by the NIHR Cambridge Biomedical Research Centre (J. H. F. R.).

Partial support was provided by: NIH/NHLBI R01 HL071021 (Z. A. F.), NIH/NHLBI R01 HL078667 (Z. A. F. and M. E. F.), and NIH/NCATS CTSA UL1TR000067 (Imaging Core) (Z. A. F.).

REFERENCES

1. Calabró P, Golia E, Maddaloni V, Malvezzi M, Casillo B, Marotta C, et al. Adipose tissue-mediated inflammation: the missing link between obesity and cardiovascular disease? Intern Emerg Med. 2009; 4:25–34. [PubMed: 19052701]
2. Grundy SM. Obesity, metabolic syndrome, and coronary atherosclerosis. Circulation. 2002; 105:2696–2698. [PubMed: 12057978]
3. Sowers JR. Obesity as a cardiovascular risk factor. Am J Med. 2003; 115(Suppl 8A):37S–41S. [PubMed: 14678864]
4. Bucerius J, Duivenvoorden R, Mani V, Moncrieff C, Rudd JH, Calcagno C, et al. Prevalence and risk factors of carotid vessel wall inflammation in coronary artery disease patients: FDG-PET and CT imaging study. JACC Cardiovasc Imaging. 2011; 4:1195–1205. [PubMed: 22093271]

5. Farb MG, Bigornia S, Mott M, Tanriverdi K, Morin KM, Freedman JE, et al. Reduced adipose tissue inflammation represents an intermediate cardiometabolic phenotype in obesity. J Am Coll Cardiol. 2011; 58:232–237. [PubMed: 21737012]
6. Apovian CM, Bigornia S, Mott M, Meyers MR, Ulloor J, Gagua M, et al. Adipose macrophage infiltration is associated with insulin resistance and vascular endothelial dysfunction in obese subjects. Arterioscler Thromb Vasc Biol. 2008; 28:1654–1659. [PubMed: 18566296]
7. Shoelson SE, Lee J, Goldfine AB. Inflammation and insulin resistance. J Clin Invest. 2006; 116:1793–1801. [PubMed: 16823477]
8. Goldfine AB, Fonseca V, Jablonski KA, Pyle L, Staten MA, Shoelson SE. The effects of salsalate on glycemic control in patients with type 2 diabetes: a randomized trial. Ann Intern Med. 2010; 152:346–357. [PubMed: 20231565]
9. Bucci M, Joutsiniemi E, Saraste A, Kajander S, Ukkonen H, Saraste M, et al. Intrapericardial, but not extrapericardial, fat is an independent predictor of impaired hyperemic coronary perfusion in coronary artery disease. Arterioscler Thromb Vasc Biol. 2011; 31:211–218. [PubMed: 21030717]
10. Rosito GA, Massaro JM, Hoffmann U, Ruberg FL, Mahabadi AA, Vasan RS, et al. Pericardial fat, visceral abdominal fat, cardiovascular disease risk factors, and vascular calcification in a community-based sample: the Framingham Heart Study. Circulation. 2008; 117:605–613. [PubMed: 18212276]
11. Sarin S, Wenger C, Marwaha A, Qureshi A, Go BD, Woomert CA, et al. Clinical significance of epicardial fat measured using cardiac multislice computed tomography. Am J Cardiol. 2008; 102:767–771. [PubMed: 18774004]
12. Gorter PM, de Vos AM, van der GY, Stella PR, Doevendans PA, Meijs MF, et al. Relation of epicardial and pericoronary fat to coronary atherosclerosis and coronary artery calcium in patients undergoing coronary angiography. Am J Cardiol. 2008; 102:380–385. [PubMed: 18678291]
13. Greif M, Becker A, von Ziegler F, Lebherz C, Lehrke M, Broedl UC, et al. Pericardial adipose tissue determined by dual source CT is a risk factor for coronary atherosclerosis. Arterioscler Thromb Vasc Biol. 2009; 29:781–786. [PubMed: 19229071]
14. Tawakol A, Migrino RQ, Bashian GG, Bedri S, Vermylen D, Cury RC, et al. In vivo 18F-fluorodeoxyglucose positron emission tomography imaging provides a noninvasive measure of carotid plaque inflammation in patients. J Am Coll Cardiol. 2006; 48:1818–1824. [PubMed: 17084256]
15. Rudd JH, Warburton EA, Fryer TD, Jones HA, Clark JC, Antoun N, et al. Imaging atherosclerotic plaque inflammation with [18F]-fluorodeoxyglucose positron emission tomography. Circulation. 2002; 105:2708–2711. [PubMed: 12057982]
16. Pedersen SF, Graebe M, Fisker Hag AM, Højgaard L, Sillesen H, Kjaer A. Gene expression and 18FDG uptake in atherosclerotic carotid plaques. Nucl Med Commun. 2010; 31:423–429. [PubMed: 20145577]
17. Christen T, Sheikine Y, Rocha VZ, Hurwitz S, Goldfine AB, Di Carli M, et al. Increased glucose uptake in visceral versus subcutaneous adipose tissue revealed by PET imaging. JACC Cardiovasc Imaging. 2010; 3:843–851. [PubMed: 20705265]
18. Virtanen KA, Lönnroth P, Parkkola R, Peltoniemi P, Asola M, Viljanen T, et al. Glucose uptake and perfusion in subcutaneous and visceral adipose tissue during insulin stimulation in nonobese and obese humans. J Clin Endocrinol Metab. 2002; 87:3902–3910. [PubMed: 12161530]
19. Tahara N, Kai H, Yamagishi S, Mizoguchi M, Nakaura H, Ishibashi M, et al. Vascular inflammation evaluated by [18F]-fluorodeoxyglucose positron emission tomography is associated with the metabolic syndrome. J Am Coll Cardiol. 2007; 49:1533–1539. [PubMed: 17418291]
20. Bucerius J, Mani V, Moncrieff C, Rudd JHF, Machac J, Fuster V, et al. Impact of Non-Insulin Dependent Type-2 Diabetes on Carotid Wall 18F-FDG-PET Uptake. J Am Coll Cardiol. 2012; 59:2080–2088. [PubMed: 22651864]
21. Rudd JH, Myers KS, Bansilal S, Machac J, Rafique A, Farkouh M, et al. (18)Fluorodeoxyglucose positron emission tomography imaging of atherosclerotic plaque inflammation is highly reproducible: implications for atherosclerosis therapy trials. J Am Coll Cardiol. 2007; 50:892–896. [PubMed: 17719477]

22. Tawakol A, Migrino RQ, Hoffmann U, Abbara S, Houser S, Gewirtz H, et al. Noninvasive in vivo measurement of vascular inflammation with F-18 fluorodeoxyglucose positron emission tomography. J Nucl Cardiol. 2005; 12:294–301. [PubMed: 15944534]
23. Williams G, Kolodny GM. Method for decreasing uptake of 18F-FDG by hypermetabolic brown adipose tissue on PET. AJR Am J Roentgenol. 2008; 190:1406–1409. [PubMed: 18430862]
24. Wang Y, Moss J, Thisted R. Predictors of body surface area. J Clin Anesth. 1992; 4:4–10. [PubMed: 1540367]
25. Rudd JH, Myers KS, Bansilal S, Machac J, Woodward M, Fuster V, et al. Relationships among regional arterial inflammation, calcification, risk factors, and biomarkers: a prospective fluorodeoxyglucose positron-emission tomography/computed tomography imaging study. Circ Cardiovasc Imaging. 2009; 2:107–115. [PubMed: 19808576]
26. Romero-Corral A, Montori VM, Somers VK, Korinek J, Thomas RJ, Allison TG, et al. Association of bodyweight with total mortality and with cardiovascular events in coronary artery disease: a systematic review of cohort studies. Lancet. 2006; 368:666–678. [PubMed: 16920472]
27. Brunken R, Freire M, Neumann D. Visceral fat volume is unrelated to adipose tissue inflammation. J Nucl Cardiol. 2008; 15 S7(Abstract).
28. Hajer GR, van Haeften TW, Visseren FLJ. Adipose tissue dysfunction in obesity, diabetes, and vascular diseases. Eur Heart J. 2008; 29:2959–2971. [PubMed: 18775919]
29. Gabrielsson BG, Johansson JM, Lönn M, Jernås M, Olbers T, Peltonen M, et al. High expression of complement components in omental adipose tissue in obese men. Obes Res. 2003; 11:699–708. [PubMed: 12805391]
30. Dusserre E, Moulin P, Vidal H. Differences in mRNA expression of the proteins secreted by the adipocytes in human subcutaneous and visceral adipose tissues. Biochim Biophys Acta. 2000; 1500:88–96. [PubMed: 10564721]
31. Virtanen KA, Iozzo P, Hällsten K, Huupponen R, Parkkola R, Janatuinen T, et al. Increased fat mass compensates for insulin resistance in abdominal obesity and type 2 diabetes: a positron-emitting tomography study. Diabetes. 2005; 54:2720–2726. [PubMed: 16123362]
32. Elkhawad M, Rudd JHF, Sarov-Blat L, Cai G, Wells R, Davies LC, et al. Effects of p38 mitogen-activated protein kinase inhibition on vascular and systemic inflammation in patients with atherosclerosis: results from a randomized controlled study. JACC Cardiovasc Imaging. 2012; 5:911–922. [PubMed: 22974804]
33. Wilson PW, D'Agostino RB, Sullivan L, Parise H, Kannel WB. Overweight and obesity as determinants of cardiovascular risk: the Framingham experience. Arch Intern Med. 2002; 162:1867–1872. [PubMed: 12196085]
34. Kotsis VT, Stabouli SV, Papamichael CM, Zakopoulos NA. Impact of obesity in intima media thickness of carotid arteries. Obesity. 2006; 14:1708–1715. [PubMed: 17062799]
35. Rogacev KS, Ulrich C, Blömer L, Hornof F, Oster K, Ziegelin M, et al. Monocyte heterogeneity in obesity and subclinical atherosclerosis. Eur Heart J. 2010; 31:369–376. [PubMed: 19687164]
36. Getz GS. Thematic review series: the immune system and atherogenesis. Immune function in atherogenesis. J Lipid Res. 2005; 46:1–10. [PubMed: 15547292]
37. Tacke F, Alvarez D, Kaplan TJ, Jakubzick C, Spanbroek R, Llodra J, et al. Monocyte subsets differentially employ CCR2, CCR5, and CX3CR1 to accumulate within atherosclerotic plaques. J Clin Invest. 2007; 117:185–194. [PubMed: 17200718]
38. Swirski FK, Libby P, Aikawa E, Alcaide P, Luscinskas FW, Weissleder R, et al. Ly-6Chi monocytes dominate hypercholesterolemia-associated monocytosis and give rise to macrophages in atheromata. J Clin Invest. 2007; 117:195–205. [PubMed: 17200719]
39. Weisberg SP, McCann D, Desai M, Rosenbaum M, Leibel RL, Ferrante AW Jr. Obesity is associated with macrophage accumulation in adipose tissue. J Clin Invest. 2003; 112:1796–1808. [PubMed: 14679176]
40. Schlitt A, Heine GH, Blankenberg S, Espinola-Klein C, Dopheide JF, Bickel C, et al. CD14+CD16+ monocytes in coronary artery disease and their relationship to serum TNF-alpha levels. Thromb Haemost. 2004; 92:419–424. [PubMed: 15269840]

41. Cottam DR, Schaefer PA, Shaftan GW, Velcu L, Angus LD. Effect of surgically-induced weight loss on leukocyte indicators of chronic inflammation in morbid obesity. Obes Surg. 2002; 12:335–342. [PubMed: 12082883]

42. Wu H, Perrard XD, Wang Q, Perrard JL, Polsani VR, Jones PH, et al. CD11c expression in adipose tissue and blood and its role in diet-induced obesity. Arterioscler Thromb Vasc Biol. 2010; 30:186–192. [PubMed: 19910635]

43. Wu H, Gower RM, Wang H, Perrard XY, Ma R, Bullard DC, et al. Functional role of CD11c+ monocytes in atherogenesis associated with hypercholesterolemia. Circulation. 2009; 119:2708–2717. [PubMed: 19433759]

44. Zhao L, Moos MP, Gräbner R, Pédrono F, Fan J, Kaiser B, et al. The 5-lipoxygenase pathway promotes pathogenesis of hyperlipidemia-dependent aortic aneurysm. Nat Med. 2004; 10:966–973. [PubMed: 15322539]

45. Lumeng CN, Bodzin JL, Saltiel AR. Obesity induces a phenotypic switch in adipose tissue macrophage polarization. J Clin Invest. 2007; 117:175–184. [PubMed: 17200717]

46. Hirata Y, Tabata M, Kurobe H, Motoki T, Akaike M, Nishio C, et al. Coronary atherosclerosis is associated with macrophage polarization in epicardial adipose tissue. J Am Coll Cardiol. 2011; 58:248–255. [PubMed: 21737014]

47. Silvera SS, Aidi HE, Rudd JH, Mani V, Yang L, Farkouh M, et al. Multimodality imaging of atherosclerotic plaque activity and composition using FDG-PET/CT and MRI in carotid and femoral arteries. Atherosclerosis. 2009; 207:139–143. [PubMed: 19467659]

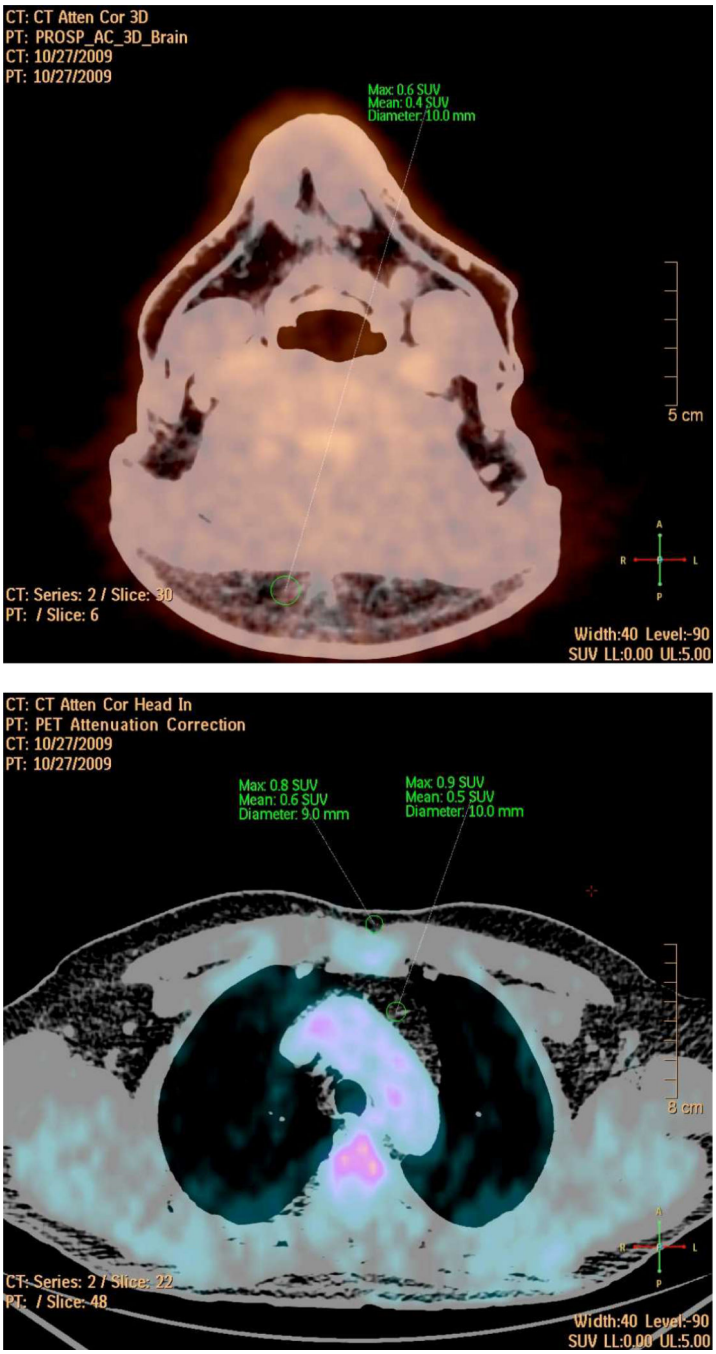

Figure 1. FDG-PET Fat Tissue Analysis

This figure shows the fused PET/CT images of the neck- (upper) and the chest region (lower) of a single patient in transaxial view. Window of the CT was set to Hounsfield units of fat tissue (−70 to −110) in order to guide the appropriate placement of the fat tissue Regions of Interest (ROIs, green).

ROIs are drawn in the subcutaneous fat tissue in the neck (NeckSub, upper) and in the presternal region (ChestSub, lower). Furthermore, ROIs were also placed in the pericardial fat tissue (ChestPeri, lower). SUV_{max}, SUV_{mean}, and diameter of the ROIs are given.

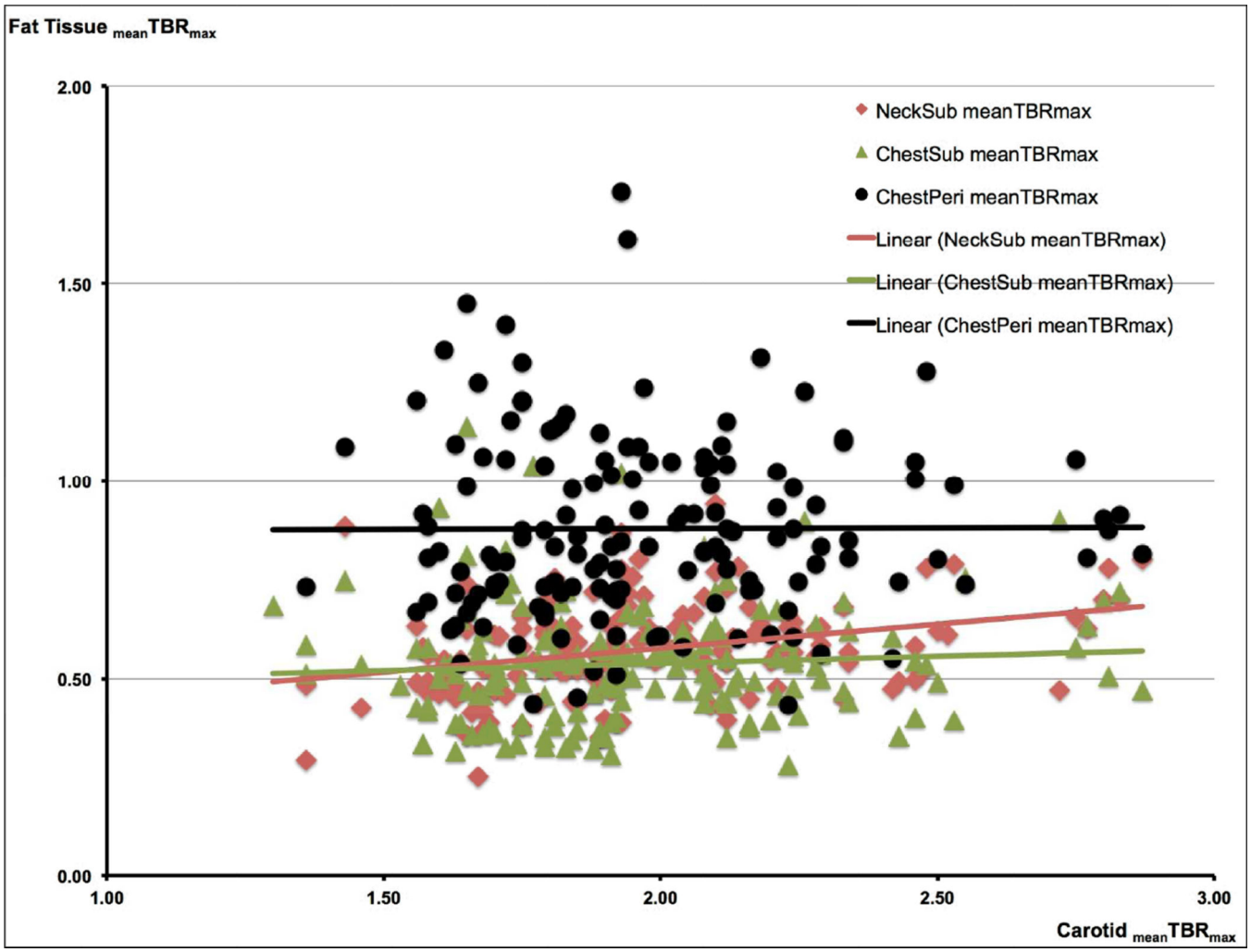

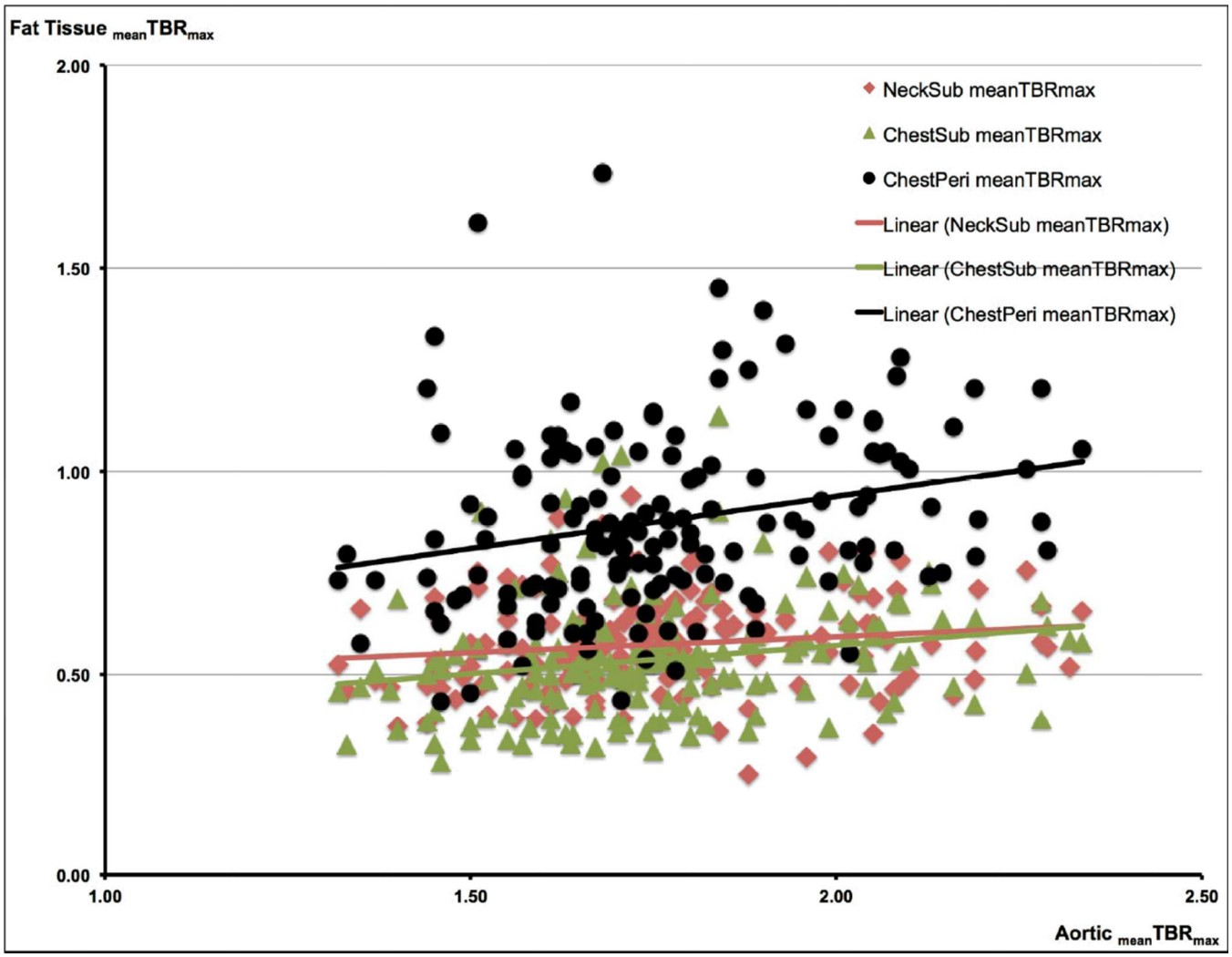

Figure 2.

a. Correlations Between the FDG Uptake in the Carotids and in the Different Fat Tissue Regions (FTRs) FDG uptake in the carotids and in the different FTRs (NeckSub, ChestSub, and ChestPeri) is given as the mean Target-to-Background ratio ($_{mean}TBR_{max}$). A significant correlation was found between carotid $_{mean}TBR_{max}$ and NeckSub $_{mean}TBR_{max}$ ($\beta = 0.262$, $p < 0.0001$). β is the standardized regression coefficient.

b. Correlations Between the FDG Uptake in the Aorta and in the Different Fat Tissue Regions (FTRs) FDG uptake in the aorta and in the different FTRs (NeckSub, ChestSub, and ChestPeri) is given as the mean Target-to-Background ratio ($_{mean}TBR_{max}$). A significant correlation was found between the aortic$_{mean}TBR_{max}$ and ChestPeri $_{mean}TBR_{max}$ ($\beta = 0.220$, $p = 0.008$) and ChestSub $_{mean}TBR_{max}$ ($\beta = 0.193$, $p = 0.019$), respectively. β is the standardized regression coefficient.

Table 1

a. Characteristics of Study Population.	
Characteristics	**n = 173**
Age (years)	56.8 ± 11.5
• Age > 65 years	45 (26.0)
Gender	
• Male	115 (66.5)
• Female	58 (33.5)
Body Mass Index (BMI; kg/m^2)	29.5 ± 5.8
• BMI < 25	34 (19.7)
• BMI ≥ 25 < 30	70 (40.5)
• BMI ≥ 30	69 (39.9)
Body Surface Area (BSA) DuBois Value	1.95 ± 0.2
Broca Value	69.2 ± 9.2
• Deviation from normal value (%)	23.0 ± 25.0
Lifestyle	
Smoking	
• Never	82 (47.4)
• Former	60 (34.7)
• Current	31 (17.9)
Alcohol Users	77 (44.5)
Exercisers	99 (57.2)
• Times per week	3.4 ± 2.4
• Time per session (min)	32.9 ± 30.4
Cardiovascular Disease	
• Myocardial Infarction	26 (15.0)
• Percutaneous Coronary Intervention	67 (38.7)
• Coronary Artery Bypass Surgery	19 (11.0)
• Stroke/Transient Ischemic Attack	11 (6.4)
• Peripheral Artery Disease	6 (3.5)
Family History of Cardiovascular Disease	98 (56.6)
Hypertension	102 (59.0)
• Duration of Hypertension (months)	112.5 ± 111.6
Diabetes	
• Diabetes Type I	6 (3.9)
• Diabetes Type II	50 (32.9)
• Duration of Diabetes (years)	5.8 ± 10.6
(Range)	0 – 58
Fasting Glucose (mmol/l)	5.9 ± 1.4
Medication	
Statin	100 (57.8)
• Duration (months)	47.0 ± 69.3

a. Characteristics of Study Population.	
Characteristics	**n = 173**
Beta-blockers	62 (35.8)
Calcium Channel Blockers	26 (15.0)
Angiotensin Converting Enzyme Inhibitors	47 (27.2)
Angiotensin II Blockers	22 (12.7)
Nitrates	7 (4.0)
Diuretics	25 (14.5)
Aspirin	92 (53.2)
Clopidrogrel	67 (38.7)
Oral Anti-Diabetics	41 (23.7)

b. FDG-PET Imaging Results.	
Patients, Total	**173**
Vascular FDG Uptake Parameters	
Carotids; n (%)	**169 (97.7)**
Number of included slices left carotid artery #	7.3 ± 2.42
Number of included slices right carotid artery #	7.0 ± 2.39
FDG uptake time (time difference between FDG injection and starting time of data acquisition; min)	137.0 ± 20.8
$_{mean}SUV_{max}$	2.21 ± 0.35
$_{mean}TBR_{max}$	1.96 ± 0.31
Aorta; n (%)	**172 (99.4)**
Number of included slices aorta #	12.3 ± 2.38
FDG uptake time (time difference between FDG injection and starting time of data acquisition; min)	101.4 ± 19.3
$_{mean}SUV_{max}$	2.14 ± 0.37
$_{mean}TBR_{max}$	1.76 ± 0.22
FDG Blood Pool Activity (Venous)	
Left and Right Jugular Vein; $_{mean}$SUV of the mean	1.14 ± 0.21
Superior Vein Cava; $_{mean}$SUV of the mean	1.22 ± 0.21
Fat Tissue FDG Uptake Parameters	
Neck, subcutaneous (NeckSub); n (%)	**153 (88.4)**
$_{mean}SUV_{max}$	0.7 ± 0.14
$_{mean}TBR_{max}$	0.57 ± 0.12
Chest, subcutaneous (ChestSub); n (%)	**168 (97.1)**
$_{mean}SUV_{max}$	0.65 ± 0.18
$_{mean}TBR_{max}$	0.54 ± 0.15
Chest, pericardial (ChestPeri); n (%)	**153 (88.4)**
$_{mean}SUV_{max}$	1.07 ± 0.29
$_{mean}TBR_{max}$	0.88 ± 0.23

Values are mean ± SD or n (%).

Values are indicated as mean ± SD and categorical data is indicated as absolute numbers and percentages. By averaging the maximum SUV values of all arterial slices of the left and right carotid artery as well as of the ascending aorta, $_{mean}$SUV values were derived for the carotid arteries and

the ascending aorta. By averaging the mean SUV values of all analyzed slices of the left and right jugular vein and the superior vena cava the $_{\text{mean}}$SUV for the FDG blood pool activities were calculated. SUV values of the carotids and the subcutaneous fat tissue in the neck are corrected for the FDG blood pool activity in the jugular veins in order to receive the TBR values, those of the aorta, the subcutaneous- and pericardial chest fat tissue for the FDG blood pool activity in the superior vein cava. TBR is the Target-to-Background-ratio.

[#]Carotid or aortic slices, which rendered sufficient and appropriate information and which were included for further analysis. Total number of analyzed slices might be higher due to exclusion of slices where appropriate placement of the arterial ROI, FDG overspill from surrounding structures into the arterial ROI, etc. could not be excluded.

Table 2

Multiple Linear Regression Analyses - Vascular FDG Uptake

Multiple Linear Regression Analyses with Backward Elimination and Enter Analysis to Identify Clinical Risk Factors of Carotid and Aortic Vessel Wall Inflammation as Depicted by FDG Uptake Parameters.

Carotids ($_{mean}TBR_{max}$)

1. **Backward Analysis**

   Explanatory Variables: **Age**, BMI, **Male Gender**, **History of Cardiovascular Disease**, **Smoking**, Alcohol, Hypertension, **Diabetes**, Family History of Cardiovascular Disease, **NeckSub $_{mean}TBR_{max}$**, ChestSub $_{mean}TBR_{max}$, ChestPeri $_{mean}TBR_{max}$

2. **Enter Analysis (only significant variables out of the Backward Analysis)**

   Explanatory Variables: Age, Male Gender, History of Cardiovascular Disease, Smoking, Diabetes, NeckSub $_{mean}TBR_{max}$

	Standardized Coefficient β	**95 % Confidence Interval**	**Adjusted R^2**	**Significance**	***p - value***
			0.235	< 0.0001	
NeckSub $_{mean}TBR_{max}$	0.262	0.309 – 1.078			< 0.0001
Age	0.209	0.001 – 0.01			0.012
Male Gender	0.182	0.017 – 0.220			0.023
History of Cardiovascular Disease	0.209	0.025 – 0.235			0.015
Diabetes	−0.215	−0.248 – −0.038			0.008

Aorta ($_{mean}TBR_{max}$)

1. **Backward Analysis**

   Explanatory Variables: **Age**, **BMI**, **Male Gender**, **History of Cardiovascular Disease**, Smoking, **Alcohol**, Hypertension, **Diabetes**, **Family History of Cardiovascular Disease**, NeckSub $_{mean}TBR_{max}$, **ChestSub $_{mean}TBR_{max}$**, **ChestPeri $_{mean}TBR_{max}$**

2. **Enter Analysis (only significant variables out of the Backward Analysis)**

   Explanatory Variables: Age, BMI, Male Gender, History of Cardiovascular Disease, Alcohol, Diabetes, Family History of Cardiovascular Disease, ChestSub $_{mean}TBR_{max}$, ChestPeri $_{mean}TBR_{max}$

	Standardized Coefficient β	**95 % Confidence Interval**	**Adjusted R^2**	**Significance**	***p - value***
			0.176	< 0.0001	
ChestPeri $_{mean}TBR_{max}$	0.220	0.056 – 0.372			0.008
ChestSub $_{mean}TBR_{max}$	0.193	0.049 – 0.542			0.019
Body Mass Index (BMI)	0.293	0.006 – 0.020			< 0.0001
Male Gender	0.212	0.023 – 0.186			0.012

The carotid and aortic mean Target-to-Background Ratios ($mean TBR_{max}$), respectively, were the response variables and the cardiovascular risk factors age, male gender, body mass index (BMI), history of cardiovascular disease, smoking, alcohol use, hypertension, diabetes, family history of cardiovascular disease as well as all of the FDG uptake parameters in the three FTRs were the explanatory variables in the Backward Elimination. Variables of these analyses were retained in the model when $p < 0.10$ (bold explanatory variables in the Backward Elimination model) and entered afterwards the ENTER Analysis (only the significant variables of the Backward Elimination are given in the table as the explanatory variables for the ENTER analysis). In that model, variables were judged to be statistically significant when $p < 0.05$. β is the standardized regression coefficient.

Table 3

Multiple Linear Regression Analyses - FDG Uptake in the Different Fat Tissue Regions (FTRs)

Multiple Linear Regression Analyses with Backward Elimination and Enter Analysis to Identify Clinical Risk Factors of FDG Uptake Parameters in Different FTRs.

NeckSub ($_{mean}TBR_{max}$)						
1.	**Backward Analysis**					
	Explanatory Variables:	Age, **BMI**, Male Gender, **BSA duBois**, Deviation from normal Broca value (%), Alcohol, Hypertension, Diabetes, Smoking				
2.	**Enter Analysis (only significant variables out of the Backward Analysis)**					
	Explanatory Variables:	BSA du Bois, BMI				
		Standardized Coefficient β	**95 % Confidence Interval**	**Adjusted R^2**	**Significance**	***p-value***
				0.118	< 0.0001	
	BSA du Bois	0.470	0.141 – 0.345			< 0.0001
	BMI	−0.284	−0.010 – −0.002			0.005
ChestSub ($_{mean}TBR_{max}$)						
1.	**Backward Analysis**					
	Explanatory Variables:	Age, **BMI**, Male Gender, **BSA duBois**, **Deviation from normal Broca value (%)**, Alcohol, Hypertension, **Diabetes**, **Smoking**				
2.	**Enter Analysis (only significant variables out of the Backward Analysis)**					
	Explanatory Variables:	BSA duBois, BMI, Deviation from normal Broca value (%), Diabetes, Smoking				
		Standardized Coefficient β	**95 % Confidence Interval**	**Adjusted R^2**	**Significance**	***p-value***
				0.090	0.001	
BSA duBois		0.619	0.043 – 0.759			0.028
Smoking		0.163	0.005 – 0.119			0.032
ChestPeri ($_{mean}TBR_{max}$)						
1.	**Backward Analysis**					
	Explanatory Variables:	Age, **BMI**, Male Gender, BSA duBois, **Deviation from normal Broca value (%)**, Alcohol, Hypertension, **Diabetes**, Smoking				
2.	**Enter Analysis (only significant variables out of the Backward Analysis)**					
	Explanatory Variables:	BMI, Diabetes, Deviation from normal Broca value (%)				
		Standardized Coefficient β	**95 % Confidence Interval**	**Adjusted R^2**	**Significance**	***p -value***
				0.058	0.008	

Deviation from normal Broca value (%)	0.978	0.001 – 0.019	0.035
Diabetes	−0.198	−0.168 – −0.020	0.013

The mean Target-to-Background Ratios ($_{mean}TBR_{max}$) of the different FTRs, respectively, were the response variables and the clinical variables age, BMI, male gender, BSA duBois, deviation from normal Broca value (%), alcohol, hypertension, diabetes, smoking were the explanatory variables in the Backward Elimination. Variables of these analyses were retained in the model when $p < 0.10$ (bold explanatory variables in the Backward Elimination model) and entered afterwards the ENTER Analysis (only the significant variables of the Backward Elimination are given in the table as the explanatory variables for the ENTER analysis). Variables were retained in the model when $p < 0.10$ and entered afterwards the ENTER Analysis. In that model, variables were judged to be statistically significant when $p < 0.05$. β is the standardized regression coefficient.